A Compact CRLH Circularly Polarized Leaky-Wave Antenna Based on Substrate-Integrated Waveguide

Mohammad Mahdi Sabahi, Abbas Ali Heidari, *Member, IEEE*, and Masoud Movahhedi, *Member, IEEE*

***Abstract*— A compact single-radiator circularly polarized (CP) leaky-wave antenna (LWA) based on composite right/left-handed (CRLH) transmission line is presented. The proposed antenna is based on substrate-integrated waveguide (SIW), and its unit cell consists of a T-shaped interdigital slot, which provides a CRLH property, a proper CP, and also effective compactness for the full-length LWA. The proposed LWA provides beam scanning from −19° to +84° over the frequency range of 7.35–10.15 GHz, while maintaining a good CP. By providing the balanced condition for the CRLH unit cell, a continuous backward-to-forward scanning including broadside is achieved. The maximum gain of the LWA is 8.95 dB which is satisfactory, considering the compactness of the antenna. Moreover, the radiation efficiency has an average of 85.7% over the operating frequency band. The measurement results are in good agreement with the simulation ones and show considerable advantages over the SIW-based CP LWAs proposed in the recent literature.**

***Index Terms*— Circular polarization (CP), composite right/left-handed (CRLH), leaky-wave antenna (LWA), substrate integrated waveguide (SIW).**

I. Introduction

LEAKY-WAVE antennas (LWAs) are basically defined as wave-guiding structures that use a traveling wave as a radiating mechanism to leak power all along the structure [1]–[3]. They have been studied for many years since the 1940s [4], and have received significant attention over the past decade [5]–[7]. Substrate-integrated waveguide (SIW) and half-mode SIW (HMSIW) have been recently favorite candidates for implementing LWAs in a low-cost, low-loss, and low-profile planar form.

Composite right/left-handed (CRLH) transmission line (TL) metamaterials are artificial and engineered media that exhibit unique electromagnetic properties not readily available in natural mediums [8]. By using CRLH structures in the LWA implementation, a backward scan can be provided for the conventional (right handed) LWAs. In addition, broadside radiation may be achieved under the balanced condition. CRLH LWAs have already been studied and developed in [9]–[12].

Recently, SIW-based circularly polarized (CP) LWAs have been under investigation using various techniques [13]–[23]. In [13] and [14], two SIW-based CP LWAs with inclined conventional slots are proposed. The unit cell structures for these antennas are depicted in Fig. 1(a) and (b), respectively.

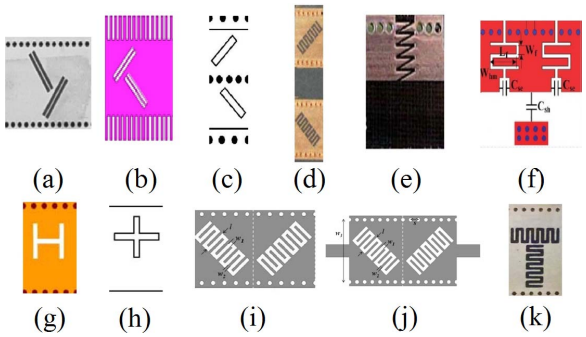

Fig. 1. Unit cell of the CP LWAs in [13]–[23]. (a) [13]. (b) [14]. (c) [15]. (d) [16]. (e) [17]. (f) [18]. (g) [19]. (h) [20]. (i) [21]. (j) [22]. (k) This paper.

Despite their advantages, the CP-radiation method may not lead to a "leaky-wave" structure with its classical meaning, for which we expect simultaneously leaking and scanning properties. In [15] and [16], using two leaky-wave radiators fed by a coupler, a CP HMSIW LWA, and a CP CRLH-SIW LWA are proposed, respectively. The essential difference between these two antennas is that conventional slots are used in [15], whereas interdigital (ID) ones are used in [16], as shown in Fig. 1(c) and (d), respectively. Therefore, for the antenna proposed in [16], a CRLH-TL structure and consequently a backward-to-forward CP scan are achieved, in contrast to that in [15]. In [17] and [18], two CP CRLH HMSIW LWAs with transverse ID slots are proposed, as shown in Fig. 1(e) and (f), respectively. The mechanism of CP radiation in both antennas is that the electric fields radiated from the transverse ID slots and the HMSIW open wall are nearly equal in magnitude and 90° out of phase. In [19], a CP SIW LWA with H-shaped typical slots is proposed, as shown in Fig. 1(g). The fundamental idea of producing CP in this antenna is that the longitudinal slot and the two transverse slots, forming the H-shaped slot, produce two perpendicular electric field components with 90° phase difference. The antenna is a planar version of a previous waveguide-based LWA with cross-shaped slots in [20], shown in Fig. 1(h). The most recent papers focusing on the compactness of CP SIW LWAs are [21] and [22]. In [22], a CP CRLH-inspired LWA is implemented using two ±45° inclined ID slots at a distance equal to a quarter wavelength in the unit cell, as shown in Fig. 1(j). A useful and brief review for the size evolution of CP CRLH LWAs is also presented by Lee and Itoh [23].

In this paper, a compact CP CRLH-SIW LWA with T-shaped ID slots is proposed. The unit cell is shown in Fig. 1(k). The CP-radiation mechanism of our antenna is similar to that of [19] and [20], in which, the conventional slots are replaced with ID ones, leading to a CRLH behavior and

Manuscript received May 24, 2017; revised April 29, 2018; accepted June 16, 2018. Date of publication June 28, 2018; date of current version August 31, 2018. *(Corresponding author: Abbas Ali Heidari.)*

The authors are with the Electrical Engineering Department, Yazd University, Yazd 89195-741, Iran (e-mail: mm.sabahi@ec.iut.ac.ir; aheidari@yazd.ac.ir; movahhedi@yazd.ac.ir).

Color versions of one or more of the figures in this paper are available online at http://ieeexplore.ieee.org.

Digital Object Identifier 10.1109/TAP.2018.2851278

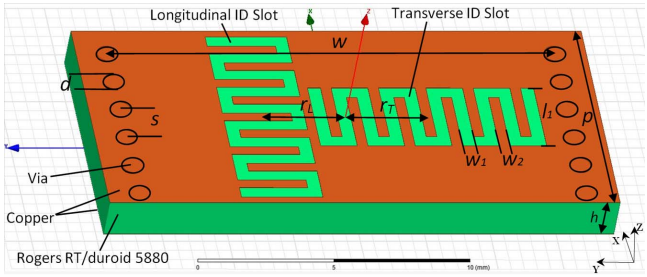

(a)

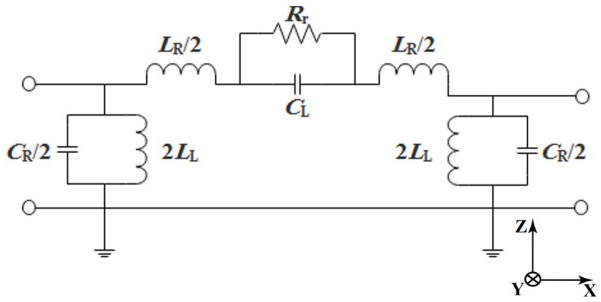

(b)

Fig. 2. (a) SIW unit cell with a transverse and longitudinal ID slots, forming a T-shaped ID slot. Slots are identical and their parameters in millimeter are: ($w_1 = 0.5$, $w_2 = 0.4$, $l_1 = 3.1$, $w = 17$, $s = 1.5$, $d = 0.8$, $p = 9.3$, $h = 1.575$, $r_L = 3.1$, $r_T = 3.05$, and $N = 9$). (b) Equivalent circuit model of the unit cell.

capability of a backward scan. To the best of the author's knowledge, this CP-radiation idea has not been used for a CRLH-SIW LWA yet. Another motivation behind using this method is to reduce the size of the CRLH unit cell; since it proposes two adjacent ID slots in the unit cell without any longitudinal spacing (unlike [22]). The proposed LWA can fulfill a continuous backward-to-forward CP scan and illuminates broadside obviously with a satisfactory gain. The CP LWA also provides the benefit of simplicity and being small since it is a single-radiator CP antenna which needs neither a second radiator nor a coupler.

This paper is organized as follows. The structure of the proposed LWA and its operating principle is illustrated in Section II. The design procedure is explained in Section III, including the design of the CRLH-SIW unit cell and the full-length antenna structure. Section IV gives a detailed description of simulation and measured results of the antenna. Last, the conclusion is drawn in Section V.

II. Proposed Structure and Operating Principle

The configuration of the LWA unit cell and its equivalent circuit model are shown in Fig. 2. The prototype of the full-length leaky-wave structure is displayed in Fig. 3. As seen in Fig. 2, the unit cell is an SIW of a short length p with two identical transverse and longitudinal ID slots on its surface, forming a T-shaped ID slot. While the ID slots are designed to radiate or "leak" power, they are expected to provide a sufficient series capacitance to realize LH structure with the aid of the inductive property of the SIW vias. Therefore, in addition to inherent RH property of the SIW, a CRLH-SIW unit cell is realized. In Fig. 2(b), an equivalent circuit model for the proposed CRLH-SIW unit cell is presented. As seen,

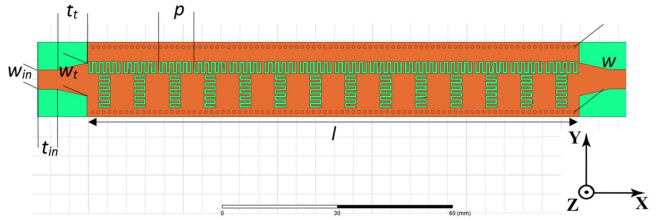

Fig. 3. Top view of the proposed LWA and its parameters in millimeter: ($w = 17$, $w_t = 8.6$, $w_{\text{in}} = 5.1$, $p = 9.3$, $l = 130.1$, $t_{\text{in}} = 5$, $t_t = 8$, and $n = 14$).

the top metal surface and the bottom metal ground of the SIW are modeled as a two-wire TL with a distributed series inductance (L_R) and shunt capacitance (C_R). This part of the model is associated with the "RH property" of an SIW. Similarly, the total series capacitance (C_L) and the shunt inductance (L_L) in the equivalent circuit model, which are provided by the ID slots and the SIW vias, respectively, represent the LH property of the unit cell. Again, the two ID slots can be modeled as a radiation resistor (R_r) from the radiation point of view. The full-length CRLH-SIW LWA is obtained by cascading 14 unit cells, as shown in Fig. 3. A piece of 50-Ω microstrip line through a tapered line is attached on each side of the entire LWA for impedance matching. The proposed CRLH LWA possesses a backward-to-forward (including broadside) scan capability as described in Sections III and IV. The scan angle of the main beam is given as follows [3]:

$$\theta = \sin^{-1}\left[\frac{\beta(\omega)}{k_0}\right] \tag{1}$$

which gives θ as a function of ω and reveals that for negative and zero values of $\beta(\omega)$, negative and zero values of θ (backward and broadside angles) can be reached, respectively.

The CP-radiation mechanism of our antenna is similar to that of the antenna proposed in [19]. In [19], a CP SIW LWA with H-shaped conventional slots is presented. The H-shaped slot cuts both the transverse and longitudinal currents on the waveguide, which are perpendicular to each other and can have 90° phase difference. From the radiation point of view, the T-shaped ID slots in our structure act the same as the H-shaped typical ones in [19]. Therefore, a CP radiation is generated as we will describe in Sections III and IV. The essential difference between our proposed structure and those in [19] and [20] is that ID or meandered slots are used here instead of conventional ones, leads to LH behavior. In fact, a meandered slot can simultaneously play a second role of a large series capacitance in a CRLH structure and is different from a conventional one, from the propagation point of view.

The proposed LWA is designed and fabricated on a Rogers RT/duroid-5880 substrate with a thickness of 62 mils (1.575 mm), a relative permittivity of 2.2, and a loss tangent of 0.0009. Other physical parameters of the antenna have been listed in Figs. 2 and 3.

III. Design Procedure

A. CRLH-SIW Unit Cell Design and Analysis

The design process must be started from the unit cell analysis, in which, the dispersion and also Bloch impedance

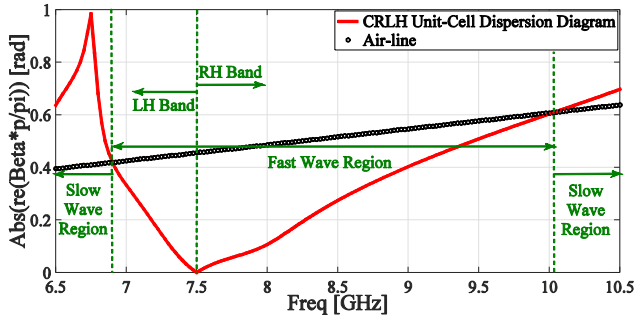

Fig. 4. Dispersion diagram for the CRLH unit cell of the proposed LWA.

diagrams of the proposed unit cell are investigated. In Fig. 4, dispersion diagram of the proposed CRLH unit cell is shown. This diagram is extracted from the S-parameters of the unit cell or by its ABCD-parameters using the following equations, respectively [8], [24], [26]:

$$\beta p = \cos^{-1}\left[\frac{1 - S_{11}S_{22} + S_{12}S_{21}}{2S_{21}}\right] \tag{2}$$

$$\beta p = \text{phase}(A \pm \sqrt{A^2 - 1}) \tag{3}$$

where p is the length of the unit cell. The dispersion curve can be extracted using the simulated S-parameters of the unit cell in high-frequency structure simulator (HFSS), either from the eigenmode simulation (by assuming the periodic boundary condition) or the fast driven-mode simulation [24]. Whereas the former is more accurate, the latter is less time consuming with a consistent result [16]. As seen in Fig. 4, the entire frequency range is separated into three regions by the plotted airline (light-line). They are two slow wave regions, also called guiding regions, above the line (freq $<$ 6.9 GHz and freq $>$ 10.04 GHz) and a fast-wave region, also called radiating or "leaky" region, below the line (6.9 GHz $<$ freq $<$ 10.04 GHz). The LH and RH radiating regions are then separated by the frequencies below and above the broadside frequency (7.5 GHz), respectively, in the fast-wave region. Verification of the LH property and also the prediction of the scan behavior for the full-length CRLH LWA are the most valuable information that can be provided from the dispersion diagram. As clearly seen in Fig. 4, there is no stopband between LH and RH radiating regions, results in a continuous backward-to-forward scan. This status is called the "balanced condition," in which the broadside radiation is guaranteed for the full-length CRLH LWA. The balanced condition for a unit cell of a CRLH TL is stated as follows [8]:

$$L_R C_L = L_L C_R \tag{4}$$

where L and C are the inductance and capacitance of the unit cell, respectively, and the subscripts R and L stand for the RH and LH property of the CRLH-TL, in turn. The LH property and the balanced condition for the unit cell are provided by adjusting the values of the series ID capacitor (C_L) and the shunt via inductance (L_L) [in Fig. 2(b)], while the RH property remains almost stable since it is associated with the nature of SIW itself. To adjust the series capacitance (C_L) according to Fig. 2, the main parameters of the ID slot, namely, length (l_1), width (w_1), and the number of fingers (N) should be tuned. Similarly, for adjusting the shunt inductance (L_L) in the SIW unit cell, we should change the parameters of the inductive vias, namely, diameter (d), length (h), and center-to-center distance (s). For example, if an increase of the shunt inductance is needed, we could have three options: decreasing d, decreasing s, and increasing h. Another way to increase L_L is to add vias near the slots, as done in [27].

The SIW design of the proposed LWA can be done using the procedures summarized into (5)–(7) [28]. Using (5)–(7), we can determine the effective width of the SIW. Then, the TE_{10} and TE_{20} cutoff frequencies are calculated about 6.11 and 12.22 GHz, respectively. Therefore, considering the fast-wave region in Fig. 4 (6.9–10.04 GHz), the LWA operates between the first and the second TE modes. Other considerations in the design process of the SIW are employing a thick substrate (62 mils) with a low permittivity (2.2) which can reduce the conductor and the dielectric losses, respectively,

$$w_{\text{eff}} = w - \frac{d^2}{0.95\ s} \tag{5}$$

$$w_{\text{eff}} = w - 1.08\frac{d^2}{s} + 0.1\frac{d^2}{w} \tag{6}$$

$$w = \frac{2\,w_{\text{eff}}}{\pi}\cot^{-1}\left(\frac{\pi\ s}{4\,w_{\text{eff}}}\ln\frac{s}{2d}\right). \tag{7}$$

Note that, at the level of unit cell design for this LWA, we should consider both features of propagation characteristic (dispersion) and radiation behavior (polarization), simultaneously. As we tune the unit cell to achieve a required dispersion (CRLH characteristic), we should not miss our radiation goal (CP). For further investigations, we should focus on the two transverse and longitudinal ID slots, forming the T-shaped ID slot in Fig. 2(a). In other words, we should investigate these ID slots separately and together, regarding both dispersion and polarization. In Fig. 5, dispersion diagrams for these slots are shown. As seen, by combining these two ID slots, a good CRLH characteristic and balanced condition are achieved (for the T-shaped ID slot). To obtain a suitable CRLH feature, we should start the design with the transverse ID slot, because it affects the dispersion diagram more than the longitudinal one (according to our parametric studies). Instead, the longitudinal ID slot is considered more than the transverse one, for tuning the CP purity of the structure (of course, it is still used to optimize the range of LH region and the position of the balanced condition). For the longitudinal ID slot individually (without the transverse one), the significant parameter which can shape the dispersion diagram and generate a CRLH behavior is r_L in Fig. 2(a). Actually, for an un-shifted ($r_L = 0$) longitudinal ID slot individually, no LH property achieved and the SIW unit cell is purely RH. Moreover, an optimum shift (r_L) is necessary for the T-shaped ID slot to produce a good CP. The polarization types of the individual ID slots and the combined one are shown in Fig. 6. As seen, the transverse ID slot individually has an X-linear polarization. It is because this slot cuts the X-component of the electric current on the SIW. Similarly, the longitudinal ID slot individually has a Y-linear polarization. Finally, for the T-shaped ID slot, CP can be produced by a proper design of the

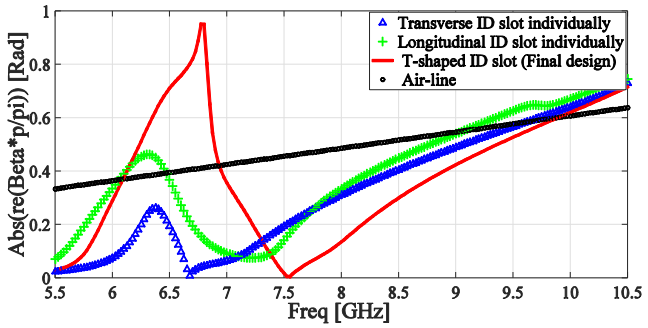

Fig. 5. Dispersion diagram for the SIW unit cell with its ID slots, individually and together.

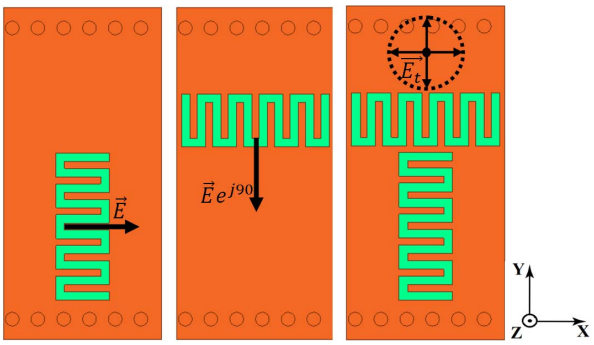

Fig. 6. Polarization status of the SIW unit cell with: (a) transverse ID slot individually. (b) longitudinal ID slot individually, and (c) T-shaped ID slot (final design).

slots for equal magnitude radiation and 90° phase difference. We will completely investigate the CP regarding polarized components of the gain and of course axial ratio (AR) for the full-length LWA in Section IV.

B. Full-Length LWA Design Considerations

For the full-length LWA, we should consider the period of putting unit cells together (p). For a traveling slot array, the spacing of the slots must not be just the half of guide wavelength (λ_g) and also a matched load must be placed at the second end of the structure [29]. In these situations, a leaky-wave structure can be realized. p is also the length of the unit cell and can influence on the LH property of the CRLH unit cell. Theoretically speaking, the length of the unit cell should be sufficiently small (usually $p < \lambda_g/4$) for an effectively homogeneous metamaterial structure to be constructed [8]. By adjusting the value of p in the allowed region, the slope of the airline ($2p \times \text{freq}/c_0$) in the dispersion diagram of the unit cell (Fig. 4) can be modified and so the fast/slow wave regions can move.

For the impedance matching of the full-length LWA, Bloch impedance diagram of the unit cell can provide helpful information, which is shown in Fig. 7. Bloch impedance can be extracted from S-parameters or ABCD parameters of the unit cell by (8) or (9), respectively, using the fast driven-mode simulation in HFSS [8], [24]

$$Z_B = \frac{2j\,Z_0\,S_{21}\sin(\beta p)}{(1-S_{11})(1-S_{22})-S_{12}S_{21}} \tag{8}$$

$$Z_B = \frac{-(A-D)\pm\sqrt{(A+D)^2-4}}{2\,C} \tag{9}$$

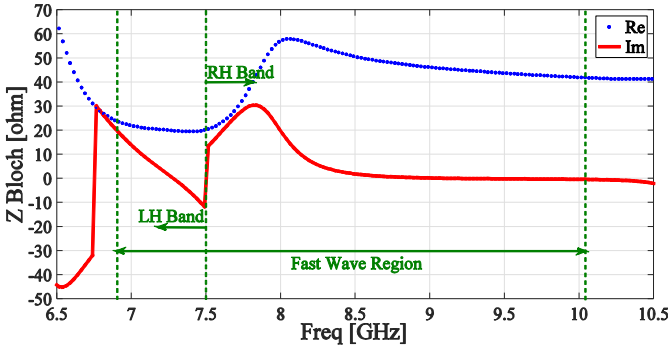

Fig. 7. Bloch impedance for the CRLH unit cell of the proposed LWA.

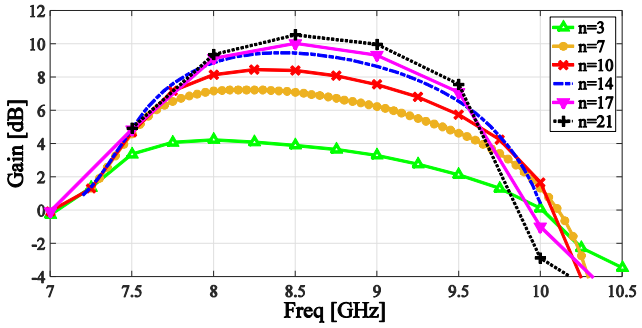

Fig. 8. Simulated gain of the proposed LWA versus frequency for several numbers of unit cells.

where Z_0 is the reference impedance of the S-matrix (here 50 Ω). The average of the real part of the Bloch impedance over the entire radiating region is calculated 41.8 Ω. This value is used to determine a proper width for a tapered line that must convert a 50-Ω microstrip line to a 41.8 Ω one. The imaginary part of the Bloch impedance is very close to zero over the RH radiating region, providing a good matching. Its negative value over the LH radiating region may be canceled by the inductive property of the SIW vias. Also, the position of the first unit cell can be changed to provide a better reactance matching.

The full-length LWA should also be long enough to leak power out efficiently (normally $10\lambda_0$ at the center of scan region [1]). For this purpose, a sufficient number of unit cells should be cascaded periodically. In Fig. 8, the gain of the antenna in the scan plane (normal plane including the array line; xz plane in Fig. 3), is plotted versus frequency and number of unit cells (n). It seems to be saturated after $n = 17$. Considering the compactness and also a satisfactory gain for the LWA, we choose 14 unit cells to be cascaded.

IV. Simulation and Measurement Results

The fabricated LWA and its S-parameters are shown in Figs. 9 and 10, respectively. As seen in Fig. 10, S_{11} is clearly below -10 dB in a wide frequency range; shows a good impedance matching. It should be noted that there is a shift of 150 MHz between the simulation and measurement results due to probably fabrication imperfections. In Fig. 10, the shifted simulated S-parameter diagram tracks the measured one satisfactorily.

We can monitor the scan behavior of the LWA in Fig. 11. According to Fig. 11, the scan region of the LWA in the scan plane is from 7.2 to 10 GHz in the simulation (7.35 to

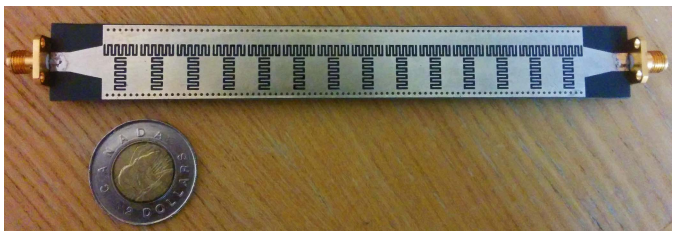

Fig. 9. Top view of the fabricated CP CRLH-SIW LWA.

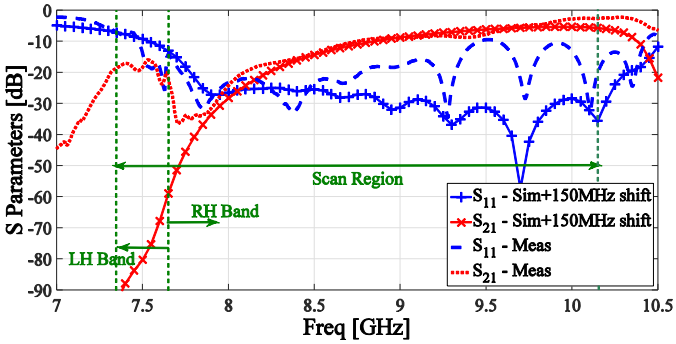

Fig. 10. S-parameters of the proposed LWA.

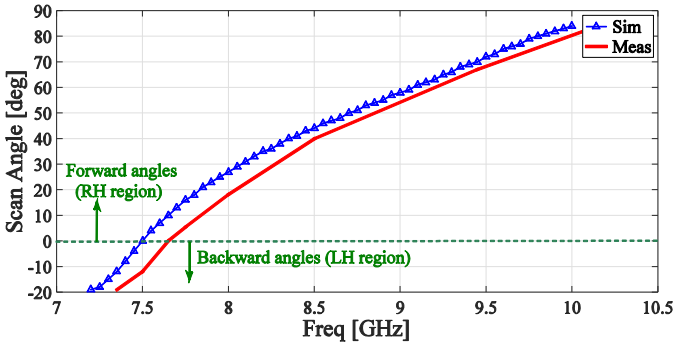

Fig. 11. Scan angle of the proposed CRLH LWA.

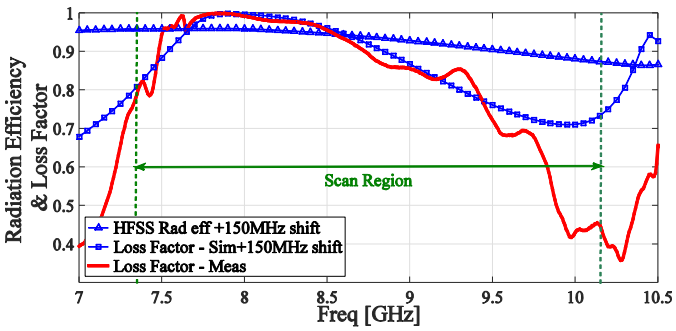

Fig. 12. HFSS radiation efficiency and Loss factor for the proposed LWA.

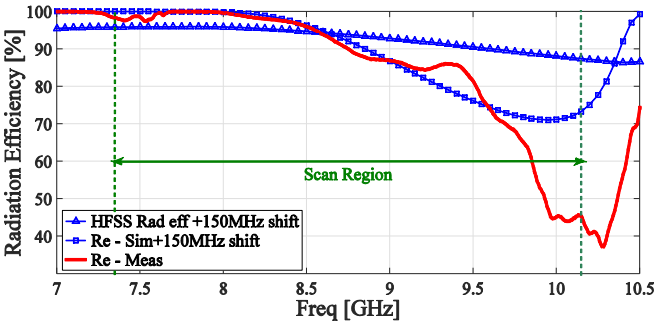

Fig. 13. HFSS radiation efficiency and *Re* for the proposed LWA.

10.15 GHz in the measurement); for which, the main beam of the antenna is scanned continuously from $\theta = -19°$ to $\theta = +84°$ without any stopband at $\theta = 0°$ (balanced condition). The maximum scan angle in the forward region of our antenna ($+84°$) is remarkable and more than the same in [13]–[19], [21], and [22]. Once again, the maximum angle of the backward scan for the LWA ($-19°$) is better than [13], [14], and [19]. In addition, the good broadside radiation in the proposed LWA is an advantage over the LWAs in [15] and [19]. The measured scan bandwidth in the LWA is 2.8 GHz (from 7.35 to 10.15 GHz) which is wider than those of [13], [14], [16], [18], [19], [21], and [22].

Achieving low S_{11} and S_{21}, while having low internal losses (dielectric and conductor losses) in the leaky structure, guarantees a good amount of radiation (external loss) through the slots. Loss factor for a 2-port TL can be defined by S-parameters using (10). Loss factor times input power equals the loss. If the loss is divided by the input power at the first port, another formula for the efficiency can be obtained in (11) [3]; where $P(0)$ is the input power at the first port and $P(L)$ is the remaining power at the end of the leaky structure. Note that the loss and loss factor in these two definitions includes internal losses in addition to the radiation. The loss factor and the new S-parameter-based efficiency (*Re*) are illustrated and compared with the simulated radiation efficiency in HFSS, in Figs. 12 and 13, respectively. As seen, the radiation efficiency is high and reaches an average of 85.8% (in the measurement) and a maximum of 96% (in the simulation) over the scan region which is better than [13], [14], [16], and [19]

$$\text{Loss factor} = 1 - |S_{11}|^2 - |S_{21}|^2 \tag{10}$$

$$R_e = 1 - \frac{P(L)}{P(0)} = \frac{(1 - |S_{11}|^2 - |S_{21}|^2)}{(1 - |S_{11}|^2)}. \tag{11}$$

The leakage (attenuation) constant of the leaky structure is defined by the S-parameters in (12) or by ABCD parameters in (13); where L is the length of the leaky structure [8], [26]. The normalized leakage constant (α/k_0) curve is shown in Fig. 14. Leakage constant as a function of frequency in the LWA concept represents the radiation per length and can usually be used to calculate the radiation efficiency as in (14). The same result as that of (11) will be obtained if (14) is used for the radiation efficiency. Note that the attenuation constant generally is the sum of all the TL losses per length and just for a loss-less TL, can be treated as the leakage constant [8]. This can be stated by (15), where α_c and α_d are attenuation constants due to conductive and dielectric losses, respectively; and α is the real leakage constant. The inconsistency of the measured and simulated normalized leakage constant at the beginning frequencies is related to the discrepancy between

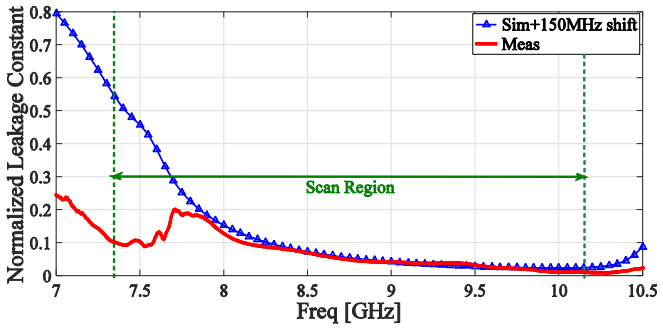

Fig. 14. Normalized leakage (attenuation) constant of the proposed LWA.

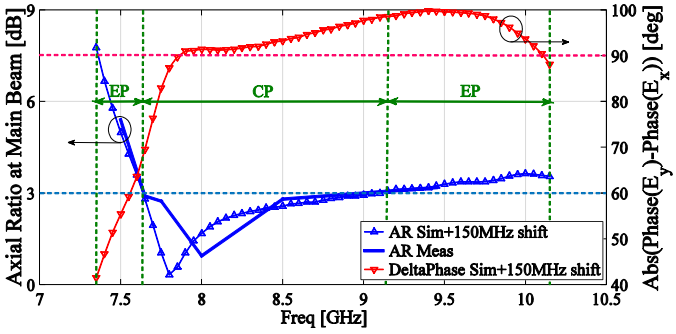

Fig. 15. AR and phase difference of the two orthogonal field components; both at the main beams of the proposed CP LWA.

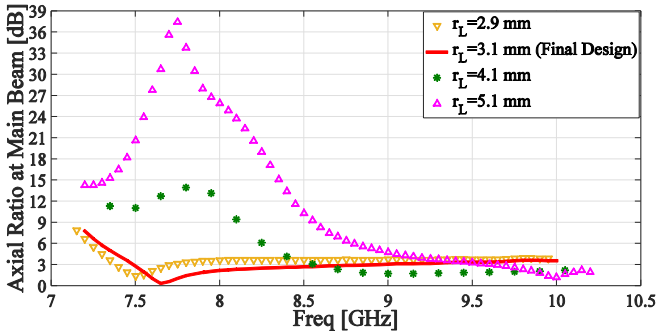

Fig. 16. AR of the proposed CP LWA at main beams as a function of r_L (longitudinal slot shift from the center line). The curve for $r_L = 3.1$ mm is the same curve that is shown in Fig.15.

the measured and simulated S_{21} which is also seen in Fig. 10

$$\alpha = \frac{-1}{2L} \ln \frac{|S_{21}|^2}{1-|S_{11}|^2} \cong \frac{-1}{L} \ln |S_{21}| \quad \text{for } |S_{11}| \ll 1 \tag{12}$$

$$\alpha = \frac{1}{L}(\ln A \pm \sqrt{A^2-1}) \tag{13}$$

$$R_e = 1 - \frac{P(L)}{P(0)} = [1 - \exp(-2\alpha L)] \tag{14}$$

$$\alpha_{\text{tot}} = \alpha + \alpha_d + \alpha_c. \tag{15}$$

One of the main features of the proposed LWA is keeping a CP, while scanned from the backward to forward. Good CP is known by an AR below 3 dB. The AR diagram along with the phase difference of the two orthogonal components (constructing the CP) at the main beams are plotted versus frequency in Fig. 15. It is apparently seen that the AR in the

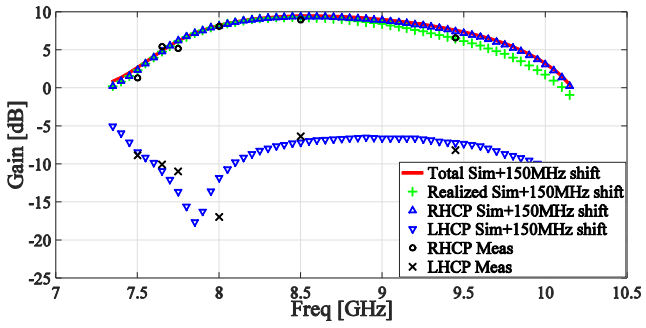

Fig. 17. Gain for the proposed CP CRLH-SIW LWA. RHCP gain is the co-pol gain and LHCP gain is the X-pol gain.

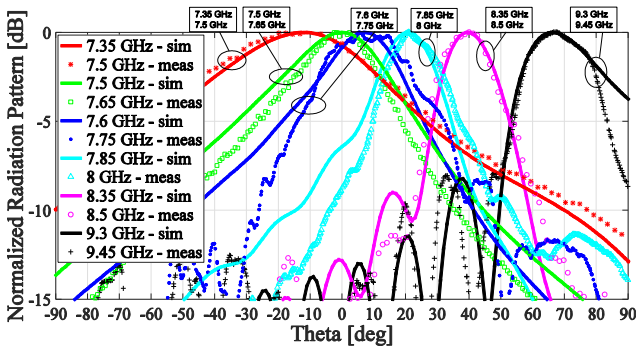

Fig. 18. Normalized radiation pattern for the proposed antenna in the scan plane for different frequencies from LH to RH ranges.

scan region is sufficiently low which confirms a good design for the CP antenna. The 3-dB AR bandwidth of the CP antenna is 1.48 GHz in the simulation (from 7.47 to 8.95 GHz) and 1.5 GHz in the measurement (from 7.63 to 9.13 GHz). The AR is below 3 dB at the broadside (7.5 GHz in the simulation and 7.65 GHz in the measurement) and increases as the scan angle moves toward the endfire or backfire of the LWA; so the CP converts to an elliptical one. This is consistent with the results of [19] using the same idea of CP radiation. The phase difference between the two orthogonal components of radiation in the forward region (7.65 to 10.15 GHz) has an average of 94.5° and a standard deviation of 4.7° that is excellent for a traveling single-radiator CP antenna. As mentioned in Section III, to adjust the CP, it is better to tune the longitudinal ID slot parameters, instead of the transverse ID slot. By changing the r_L, [refer to Fig. 2(a)], the designer can optimize both the phase difference and the magnitude ratio of the two perpendicular components of radiation (according to our parametric studies). Fig. 16 shows the AR of the full-length LWA at main beams as a function of r_L. It shows that we can control the CP quality by tuning the position of longitudinal ID slot.

A complete comparison between the experimental characteristics of the proposed LWA and some of the recent SIW-based CP LWAs are gathered into Table I. In Table I, the electrical size is the real size divided by the unbounded wavelength at the center frequency $(\lambda_0/(\varepsilon_r)^{1/2})$. Some of the information in Table I which is not stated explicitly in the related papers is carefully collected from their associated figures and tables.

TABLE I
REVIEW OF CP SIW-BASED LWAS IN THE RECENT LITERATURE

Antenna	LWA Type					CP-Radiation Idea	Scan Coverage (θ) (in a same coordinate)	Broadside Radiation	Scan BW (GHz) (%)	Scan Type	Polarization	3-dB CP BW (GHz)	Number of Unit-cells	Electrical Length: W * L (without feed line) (λ)	Max Gain (dBi)	Max Rad Eff. (%)
	Fabrication Technology	TL Type	Slots: Type	Slots: Geometry	Using											
[13]	SIW	RH	Typical	±45° Inclined	-	Two paired of slots	(-2 , +2)	Yes	(15.8 - 16.2) 2.5	Frequency (limited)	CP	Very limited	16	1.7 * 22.5	18.9	93.3
[16]	SIW	CRLH	ID	±45° Inclined in Two Antennas	Coupler	Two Slotted Antenna	(-30 , +50) CP mode	Yes	(7.5 - 10) 28.6 CP mode	Frequency	LP & CP	(7.5 - 10)	14	1.5 * 5.6 (also without coupler)	12 LP mode	80 LP mode
[18]*	HMSIW	CRLH	ID	Transverse	Varactor Diode	Slot + Open Wall of HMSIW	(-31 , +35)	Yes	Very limited around 6.5 GHz	Electronic (Fixed frequency)	CP	Very limited	15	6.1* NR (HMSIW)	9.89	NR
[19]	SIW	RH	Typical	H shaped	-	Three slots	(+8 , +75)	No (But close)	(9.9 – 11.7) 16.7	Frequency	CP	(10.3 – 10.5)	42	2.7 * 15.1	15.8	60
[22]	SIW + M_line	CRLH-Inspired	ID	±45° Inclined (with λ/4 spacing)	-	Two slots	(-25 , +26)	Yes	(4.2 – 4.85) 14.4	Frequency	CP	(4.2 – 4.85)	5	4.2 * 50.3 (W is related to SIW)	2.5	NR
This Work	**SIW**	**CRLH**	**ID**	**T shaped**	-	**Two slots**	**(-19 , +84)**	**Yes**	**(7.35 - 10.15) 32**	**Frequency**	**CP**	**(7.63 – 9.13)**	**14**	**0.8 * 5.6**	**8.95 dB**	**Max: 96 Av: 85.8**

*: Simulation Results

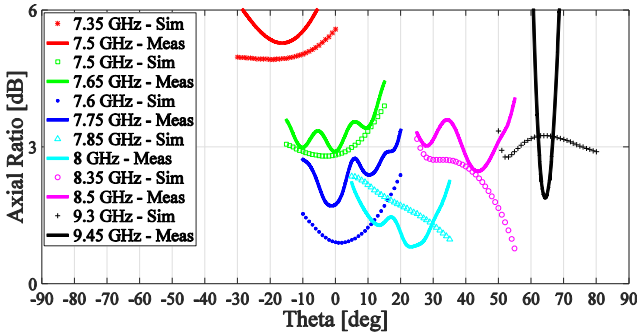

Fig. 19. AR of the proposed antenna in the scan plane for different frequencies from LH to RH ranges.

In Fig. 17, the gain and realized gain are plotted versus frequency. As seen, the RHCP gain (co-pol gain here) coincides with the total gain satisfactorily. This means the CP of the antenna is RH. On the other hand, the LHCP gain (X-pol gain here) is suitably lower than the total gain. According to Figs. 3 and 9, if the antenna is fed at the left port, the polarization of the antenna will be RHCP and vice versa. The maximum gain of the antenna is 8.95 dB in the measurement (9.47 dB in the simulation) and increases to 11 dB in the simulation by increasing the length of the antenna and adding more slots (refer to Fig. 8).

The normalized pattern and the AR for different frequencies (associated with the backward, broadside, and forward angles) in the scan plane are depicted in Figs. 18 and 19, respectively. The main beam of the antenna is scanned continuously from $\theta = -19°$ to $\theta = +84°$ with the increase of frequency. These beams have an elliptical polarization in the backward and a CP at the broadside and forward of the antenna. As noted before, in Fig. 18 and all of our results, there is a shift of about 150 MHz between the simulation and the measurement. If we look at both Figs. 18 and 19 simultaneously, we will see that minimums of the AR curve at each frequency take almost place at the angles of maximum radiation, where is ideal.

V. CONCLUSION

The design and implementation of a compact single-radiator CP LWA based on a CRLH-SIW are presented. T-shaped ID slots are used for CRLH-TL realization and CP radiation. The CP radiation method has led to a compact $0.8\lambda \times 5.6\lambda$ CP CRLH LWA with a continuous scan from $-19°$ to $+84°$ over the frequency range of 7.35 to 10.15 GHz. The proposed CP LWA needs neither a second radiator nor a coupler and so has a simple structure. Performance of the fabricated LWA shows considerable advantages over the recent SIW-based CP LWAs in size, scan capability, and radiation efficiency. It is a talented antenna candidate for wireless applications with CP backward-to-forward scanning requirements.

REFERENCES

[1] T. Tamir, "Leaky-wave antennas," in *Antenna Theory, Part II*, R. E. Collin and F. J. Zucker, Eds. New York, NY, USA: McGraw-Hill, 1969, Ch. 20.

[2] C. A. Balanis, Ed., "Leaky-wave antennas," in *Modern Antenna Handbook*, vol. 1. Hoboken, NJ, USA: Wiley, 2008, pp. 325–368.

[3] A. A. Oliner and D. R. Jackson, "Leaky-wave antennas," in *Antenna Engineering Handbook*, J. L. Volakis, Ed., 4th ed. New York, NY, USA: McGraw-Hill, 2007, Ch. 11.

[4] W. W. Hansen, "Radiating electromagnetic wave guide," U.S. Patents 2 402 622 A, Jun. 25, 1946.

[5] D. R. Jackson, C. Caloz, and T. Itoh, "Leaky-wave antennas," *Proc. IEEE*, vol. 100, no. 7, pp. 2194–2206, Jul. 2012.

[6] F. Xu and K. Wu, "Understanding leaky-wave structures: A special form of guided-wave structure," *IEEE Microw. Mag.*, vol. 14, no. 5, pp. 87–96, Jul. 2013.

[7] F. Monticone and A. Alù, "Leaky-wave theory, techniques, and applications: From microwaves to visible frequencies," *Proc. IEEE*, vol. 103, no. 5, pp. 793–821, May 2015.

[8] C. Caloz and T. Itoh, *Electromagnetic Metamaterials: Transmission Line Theory and Microwave Applications*. Hoboken, NJ, USA: Wiley, 2005.

[9] C. Caloz, T. Itoh, and A. Rennings, "CRLH metamaterial leaky-wave and resonant antennas," *IEEE Antennas Propag. Mag.*, vol. 50, no. 5, pp. 25–39, Oct. 2008.

[10] M. R. M. Hashemi and T. Itoh, "Evolution of composite right/left-handed leaky-wave antennas," *Proc. IEEE*, vol. 99, no. 10, pp. 1746–1754, Oct. 2011.

[11] Y. Dong and T. Itoh, "Metamaterial-based antennas," *Proc. IEEE*, vol. 100, no. 7, pp. 2271–2285, Jul. 2012.

[12] C. Caloz, "Metamaterial dispersion engineering concepts and applications," *Proc. IEEE*, vol. 99, no. 10, pp. 1711–1719, Oct. 2011.

[13] P. Chen, W. Hong, Z. Kuai, and J. Xu, "A substrate integrated waveguide circular polarized slot radiator and its linear array," *IEEE Antennas Wireless Propag. Lett.*, vol. 8, pp. 120–123, 2009.

[14] C. Liu, Z. Li, and J. Wang, "A new kind of circularly polarized leaky-wave antenna based on corrugated substrate integrated waveguide," in *Proc. IEEE 5th Int. Symp. Microw., Antenna, Propag. EMC Technol. Wireless Commun. (MAPE)*, Oct. 2013, pp. 383–387.

[15] Y. J. Cheng, W. Hong, and K. Wu, "Millimeter-wave half mode substrate integrated waveguide frequency scanning antenna with quadri-polarization," *IEEE Trans. Antennas Propag.*, vol. 58, no. 6, pp. 1848–1855, Jun. 2010.

[16] Y. D. Dong and T. Itoh, "Substrate integrated composite right-/left-handed leaky-wave structure for polarization-flexible antenna application," *IEEE Trans. Antennas Propag.*, vol. 60, no. 2, pp. 760–771, Feb. 2012.

[17] A. Pourghorban Saghati, M. M. Mirsalehi, and M. H. Neshati, "A HMSIW circularly polarized leaky-wave antenna with backward, broadside, and forward radiation," *IEEE Antennas Wireless Propag. Lett.*, vol. 13, pp. 451–454, 2014.

[18] A. Suntives and S. V. Hum, "A fixed-frequency beam-steerable half-mode substrate integrated waveguide leaky-wave antenna," *IEEE Trans. Antennas Propag.*, vol. 60, no. 5, pp. 2540–2544, May 2012.

[19] J. Liu, X. Tang, Y. Li, and Y. Long, "Substrate integrated waveguide leaky-wave antenna with h-shaped slots," *IEEE Trans. Antennas Propag.*, vol. 60, no. 8, pp. 3962–3967, Aug. 2012.

[20] W. J. Getsinger, "Elliptically polarized leaky-wave array," *IRE Trans. Antennas Propag.*, vol. 10, no. 2, pp. 165–171, Mar. 1962.

[21] H. Lee, J. H. Choi, Y. Kasahara, and T. Itoh, "A circularly polarized single radiator Leaky-wave antenna based on CRLH-inspired substrate integrated waveguide," in *IEEE MTT-S Int. Microw. Symp. Dig.*, Jun. 2014, pp. 1–3.

[22] H. Lee, J. H. Choi, C.-T. M. Wu, and T. Itoh, "A compact single radiator CRLH-inspired circularly polarized leaky-wave antenna based on substrate-integrated waveguide," *IEEE Trans. Antennas Propag.*, vol. 63, no. 10, pp. 4566–4572, Oct. 2015.

[23] H. Lee and T. Itoh, "Evolution of circularly polarized composite right/left-handed leaky-wave antenna," in *Proc. Asia–Pacific Microw. Conf. (APMC)*, Nov. 2014, pp. 134–136.

[24] *Left-Handed Metamaterial Design Guide*, Ansoft Corp., Pittsburgh, PA, USA, 2007.

[25] Y. D. Dong and T. Itoh, "Composite right/left-handed substrate integrated waveguide and half mode substrate integrated waveguide leaky-wave structures," *IEEE Trans. Antennas Propag.*, vol. 59, no. 3, pp. 767–775, Mar. 2011.

[26] O. Vanbésien, *Artificial Materials*. Hoboken, NJ, USA: Wiley, 2012.

[27] S. S. Haghighi, A. A. Heidari, and M. Movahhedi, "A three-band substrate integrated waveguide leaky-wave antenna based on composite right/left-handed structure," *IEEE Trans. Antennas Propag.*, vol. 63, no. 10, pp. 4578–4582, Oct. 2015.

[28] M. Bozzi, A. Georgiadis, and K. Wu, "Review of substrate-integrated waveguide circuits and antennas," *IET Microw. Antennas Propag.*, vol. 5, no. 8, pp. 909–920, Jun. 2011.

[29] R. S. Elliott, *Antenna Theory & Design*. Piscataway, NJ, USA: IEEE Press, 2003.

Mohammad Mahdi Sabahi received the B.S. degree in communication engineering from the Isfahan University of Technology, Isfahan, Iran, in 2012, and the M.S. degree in communication engineering from Yazd University, Yazd, Iran, in 2015.

Since 2015, he has been a Graduate Student Researcher with the Department of Electrical and Computer Engineering, Isfahan University of Technology. His current research interests include the development of RF and microwave components, circuits, metamaterials, leaky-wave antennas, and phased array antennas.

Abbas Ali Heidari (M'09) was born in Yazd, Iran, in 1970. He received the B.Sc. degree in electrical engineering from the Shahid Bahonar University of Kerman, Kerman, Iran, in 1993, and the M.Sc. and Ph.D. degrees in electrical engineering from Tarbiat Modarres University, Tehran, Iran, in 1996 and 2003, respectively.

He was the Head of the Electrical Engineering Department, Yazd University, Yazd, Iran, from 2004 to 2006, the Dean of the E-Learning and Open Learning Center from 2007 to 2010, the Head of the Technology Affairs from 2014 to 2016, and currently an Associate Professor and the Head of the Communication Engineering Department. His current research interests include computational electromagnetic, microstrip antennas, metamaterial structures, and microwave components and circuits.

Masoud Movahhedi (S'06–A'07–M'08) was born in Yazd, Iran, in 1976. He received the B.Sc. degree in electrical engineering from the Sharif University of Technology, Tehran, Iran, in 1998, and the M.Sc. and Ph.D. degrees in electrical engineering from the Amirkabir University of Technology, Tehran, in 2000 and 2006, respectively.

In 2005, he joined the Institute for Microelectronics, Technische Universität Vienna, Vienna, Austria, as a Visiting Student. He is currently an Associate Professor with the Electrical Engineering Department, Yazd University, Yazd, Iran. His current research interests include the computer-aided design of microwave integrated circuits, computational electromagnetic, semiconductor high-frequency RF modeling, and metamaterials.

Dr. Movahhedi was a recipient of the GAAS-05 Fellowship sponsored by the GAAS Association to young graduate researchers for his paper presented at GAAS2005 and the Electrical Engineering Department Outstanding Student Award in 2006.